# Silicon Grisms and Immersion Gratings Produced by Anisotropic Etching: Testing and Analysis

Jasmina P. Marsh[a], Oleg A. Ershov[a], and Daniel T. Jaffe[a]

[a]University of Texas at Austin, Department of Astronomy, Austin, TX 78712

## ABSTRACT

Because they can vastly reduce the required collimated beamsize at a given diffraction-limited resolution, silicon immersion gratings and grisms are an enabling technology for high resolution infrared spectroscopy from space and are highly useful in a range of ground-based and airborne instruments. We have used anistropic etching techniques to produce diffraction gratings on bulky silicon substrates. These devices can serve as high resolution grisms (when used in transmission), as coarse front-surface gratings, or as very high resolution immersion gratings. We have been able to produce devices with high optical efficiency by insuring that their entrance faces and groove surfaces are optically flat and that the groove positions are correct to within tolerance appropriate to the wavelength where the gratings will be used.

We report here on testing and evaluation of high resolution Si gratings both in transmission (grism) and in reflection (immersion) mode.

**Keywords:** silicon, micromachined, diffraction gratings, IR testing

## 1. INTRODUCTION

Silicon diffraction gratings and grisms are very useful devices in the infrared because they can be compact and still maintain high resolving power. The wavelength of light in silicon is n=3.4 times shorter than in air. When silicon diffraction gratings are used as immersion devices (light passing through the silicon prism before being diffracted by the grating and then leaving the prism through the same entrance face), the resolving power, R=($\lambda/\Delta\lambda$), of such a grating scales with n:

$$\mathrm{R} = \frac{2\ \mathrm{n}\ \mathrm{L}\ \sin\ \delta}{\lambda} \tag{1}$$

where L is the length of the illuminated part of the grating and $\delta$ is the blaze angle. If we want to obtain the same resolving power as with a standard, front-surface grating, we can make the silicon grating 3.4 times shorter (and a collimated beam 3.4 times narrower) which will result in a significant reduction in the volume and therefore mass of our spectrometer. On large telescopes, where the overall spectrometer throughput at a given resolution is often driven by the mismatch between the slit size and the size of the seeing disk, an immersion grating spectrometer with the same size grating as a conventional instrument with the same R, can have a slit that is n times wider on the sky.

For a grism, the resolution scales with n-1:

$$\mathrm{R} = \frac{(\mathrm{n}-1)\ \mathrm{L}\ \sin\ \delta}{\lambda}. \tag{2}$$

so a silicon grism would have a resolving power advantage ranging from a factor of $\sim$1.8 (compared to KRS-5; n$\sim$2.4) to a factor of $\sim$4.8 (compared to a glass grism; n$\sim$1.5) with the same (or similar) dimensions. As with the immersion gratings, we can use this advantage to either design a smaller grism or one with higher resolving power. In addition to the gain in resolving power we would realize from the use of silicon, the anistropic etching of the grating grooves offers two possible advantages. The first is that the etching process produces almost

Further author information: (Send correspondence to J.P. Marsh)
J.P. Marsh: E-mail: jasna@astro.as.utexas.edu

perfectly flat and smooth groove walls, properties that are especially important for efficiency in high orders where loss of power into nearby orders is a potential problem.[1] This high groove quality may not be achievable when ruling or machining other high-index materials. The second advantage is that etching allows us to produce much coarser grooves than can be made by ruling. This capability is important for long wavelength grisms and for devices to be used in high order or with small detectors. The high quality of the groove walls and the possibility of making coarse grooves can also make etched gratings preferable in some applications calling for conventional, front-surface gratings.

When producing infrared dispersive elements by anisotropic etching of silicon, the difference between a grism, an immersion grating and a front-surface grating is in the basic design (groove period and blaze angle) and in coatings (e.g. immersion grating will have an AR coating on its entrance face and a reflective coating on the grooves whereas a grism will have AR coatings on both the grooves and the entrance face). For purposes of testing, however, a single (uncoated) grating can be used in all three modes. We haved recently produced a prototype grating[1] suitable for optical evaluation in all three modes. The grating was etched on an optically flat disk (15 mm thick, 70 mm in diameter). It has symmetric grooves spaced at 142 $\mu$m (Figure 1 right). We contracted Janos Technologies Inc. to cut the disk into a prism and optically polish the entrance face. The prism (Figure 1 left) has a 54.7° opening angle so the grating has a 54.7° blaze angle. The entrance face is 17 mm x 42 mm and the grating surface etched into the hypotenuse of the prism is 30 mm x 42 mm. The device was tested previously as a front-surface grating using two HeNe lasers (red at 632 nm and green at 543 nm).[1] We reported 70% efficiency at 632 nm, consistent with a 37 nm RMS error in groove spacing (the estimated RMS error in groove spacing from interferograms was 30 nm). The prism was left uncoated with the intention of testing the grating in immersion and transmission in the infrared at a later date.

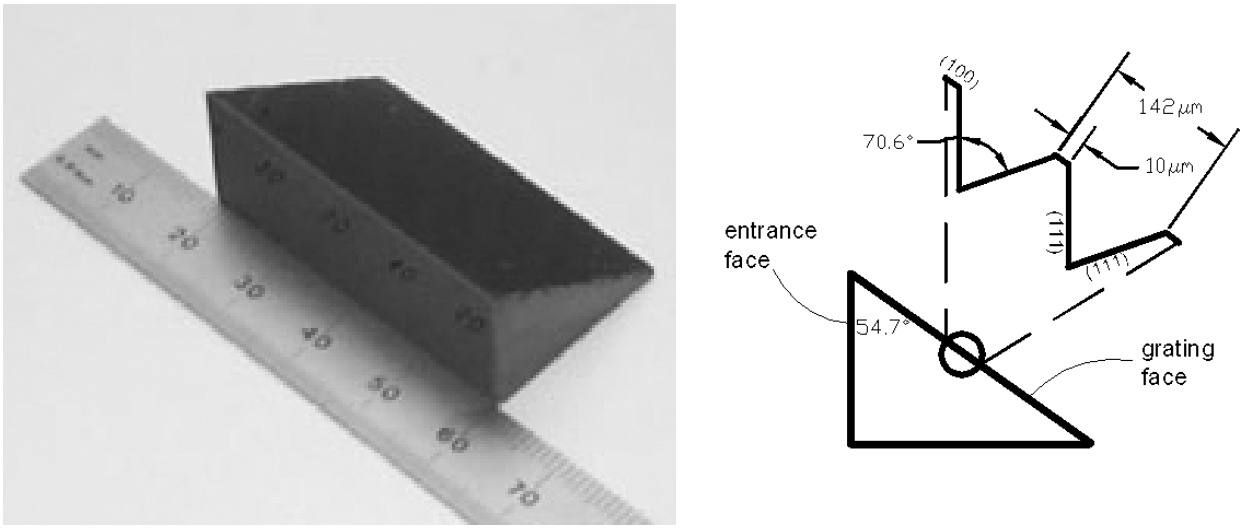


**Figure 1.** (left) Sample prism used in this work for evaluation of our manufacturing process.[1] The prism opening angle is 54.7°. The entrance face (the side facing the ruler) is 17 mm x 42 mm and the hypotenuse face, which is 30 mm x 42 mm, has the grating etched into it. The grating pattern consists of symmetric grooves with a 142 $\mu$m period. (right) Illustration showing the prism and the groove profile. Grooves are symmetric with an opening angle 70.6°. The groove period is 142 $\mu$m and the groove tops are 10 $\mu$m wide (artifacts of the process used to make the grating.[2] )

## 2. TESTING SETUP

Silicon is opaque at optical wavelengths. Until now, we have only been able to test our gratings as front-surface devices and make indirect conclusions about their performance as immersion gratings and grisms.[1,3] However, we recently acquired an Alpha NIR camera (320 x 256 InGaAs array with 30 $\mu$m square pixels

sensitive in the 0.9–1.7 $\mu$m region) from Indigo Systems which allowed us to expand our tests into the near-infrared. The thermoelectrically cooled detector operates after only a short cooldown time and focusing is made straightforward by a real-time image display.

Figure 2 illustrates the optical setups used to produce the spectra we evaluate here. In the reflection (immersion) mode, the grating to be tested is positioned in Arm 2 and a reference mirror in Arm 1. The reflection from the reference mirror and the spectrum from the grating are offset slightly in angle and both focused by a camera lens (usually of focal length 200 mm) onto the camera. In the transmission mode, there is no Arm 2 and the light reflected from the mirror in Arm 1 passes through the grism on the way to being focused by the camera lens onto the detector. In this mode, the reference signal is obtained in a separate exposure after removing the test sample from the beam.

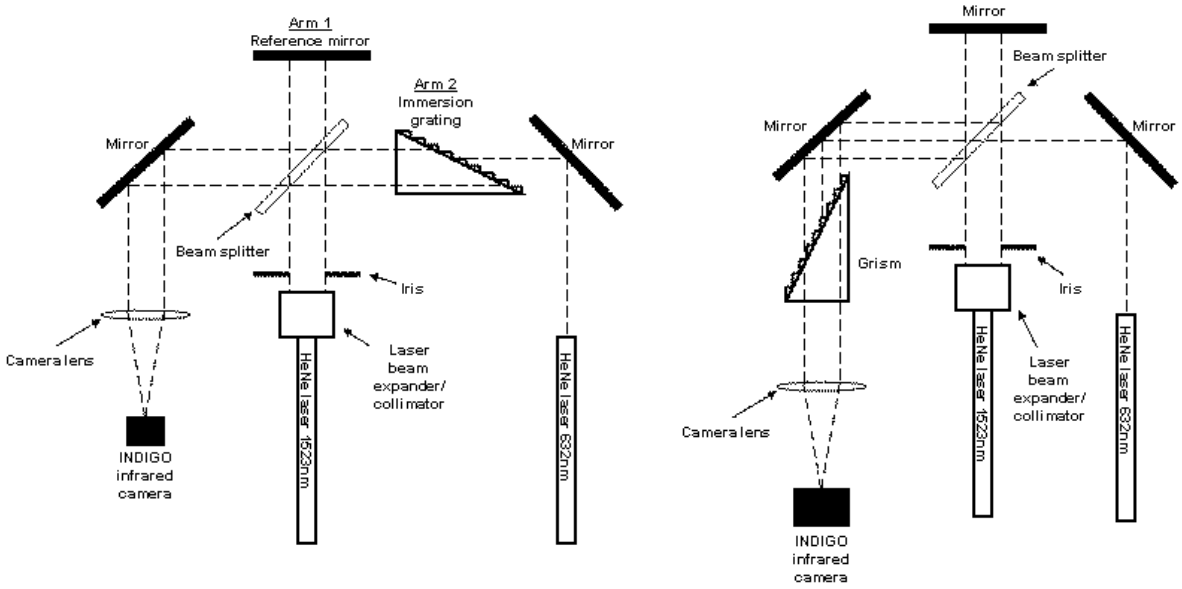


**Figure 2.** Test setup for immersion grating/front-surface grating (left) and grism (right). In both cases, the light source is an IR HeNe laser at 1.523 $\mu$m with a collimator producing a 10 mm beam. After passing through the beam splitter, the light is reflected by the reference mirror in Arm 1 or diffracted by an immersion or front-surface grating in Arm 2. In the grism mode, there is no Arm 2 and light passes through the grism on the way to the detector. The red HeNe laser was used for alignment.

We use a HeNe laser at 1.523 $\mu$m as a light source for our spectrometer setup and a red HeNe laser at 632 nm for alignment. First, we aligned the IR laser and all the optical elements in the light path to make the beam parallel to the optical bench surface and centered on the detector. Then we aligned the red HeNe laser beam to coincide with the optical discharge from the IR laser and made sure it was still parallel to the surface. We had to observe the discharge from the IR laser and position the red beam in the center of the collimated discharge representing the IR beam by eye since the IR camera cannot detect light at 632 nm. When test pieces are inserted into the setup, we insure that the gratings operate in Littrow by orienting them so that the principal order at 632 nm returns to the entrance aperture of the red HeNe laser. We are now able to use reflected red light for alignment in the reflection mode or diffracted red light in the immersion/transmission mode. Because the entrance face is cut at a small offset ($\sim$1°) from the direction parallel to the grooves in order to redirect reflected light, we had to rotate the grating through a small angle to ensure the grating was in Littrow when operating in the reflection mode. This extra step was avoided in the grism mode by turning the grism so that light hits the grating side first allowing us to align diffracted red light from the grism with the incoming red beam.

Science images are stored on the host computer in datasets which include raw data as well as three arrays containing non-uniformity corrections and a bad pixel table. Images were corrected (gain, bias and bad pixel corrections) using the algorithm supplied by Indigo Systems and then saved as 2D FITS images for further analysis with IDL. Exposures were also taken with the laser turned off in order to remove background intrinsic to the camera. The first step in analysis was to subtract this background from all 2D images. The dispersion direction is along the rows of the camera so we summed 30-40 pixels along columns to get a 1D spectrum. Diffuse background is removed at this point by interactively fitting a line to the selected parts of the spectrum (usually close to endpoints) and the spectrum is then saved in FITS format.

## 3. RESULTS

We made throughput measurements in all three modes using an uncoated, polished silicon prism as a reference mirror since none of the grating surfaces had been coated. The performance of our grating in all modes was determined by integrating intensity in all observed orders and comparing this value to the reflection from the silicon mirror (the reflectivity of a single silicon surface at normal incidence is 30.6%). The measured arm coefficient of 1.09 (the difference in the return loss for the two arms due to the slightly different incidence angles of the reflected beams at the beamsplitter) was used to correct all measurements in immersion/reflection but not for grism measurements since there was no Arm 2 in transmission. The summary of measurements and predicted performances is given in Table 1. The measurement errors mostly result from uncertainties in the arm coefficient measurements. The upper bound on arm coefficient measurement error is 3.0%. The absorption coefficient for silicon is 0.0103 $cm^{-1}$ (at 290 K) resulting in 0.86% of incident light being absorbed by a silicon disk 10 mm in thickness.[4] The error in our calculation resulting from neglecting absorption in silicon is then 1.7% for immersion and 0.9% for transmission.

**Table 1.** Measured throughputs at 1.523 $\mu$m compared to a silicon grism (front surface reflectivity of 30.6% for normal incidence). Predicted $\eta/\eta_0$ values given in the last column are based on the RMS spacing error of 37 nm calculated from the measured throughput at 632 nm.

| Mode | Measured throughput ($\eta$) | Ideal throughput ($\eta_0$) (calculated) | Measured $\eta/\eta_0$ | Predicted $\eta/\eta_0$ for $\Delta\sigma_{rms}$=37 nm[1] |
|---|---|---|---|---|
| Reflection (at 632 nm)[1] | 70.0 | 93.0 | 76.3 | 76.3 |
| Reflection | 85.5 | 93.0 | 91.8 | 95.4 |
| Immersion | 25.9 | 48.2 | 53.7 | 56.8 |
| Transmission | 30.5 | 28.1 | 108.5 | 93.1 |

When used as a front surface grating, our device had net throughput of 85.5%±3.0% in three orders at 1.523 $\mu$m. This measurement is compared to an ideal throughput of $\eta_0$=93% (values given in column 3 of Table 1). The value of $\eta_0$ differs from 100% because of losses resulting from shadowing by groove tops which effectively constitute a grating blazed at 0° thus removing 7% of light from the spectrum. Table 1 also lists a throughput predicted based on an RMS error in the groove positions of 37 nm (column 5). This value was derived from the reflection throughput measurements at 632 nm[1] listed in the first row of the table. The difference between the measured relative throughput of 91.8% and predicted value of 95.4% is consistent with the measurement error for the grating in reflection. Since our grating is not blazed at exactly 1.523 $\mu$m, we calculated the throughput of our grating for monochromatic light at the blaze wavelength[5] and got 57%.

In transmission, the measured throughput was 30.5%±0.9% in four orders at 1.523 $\mu$m. The large blockage from the adjacent grooves at the blaze angle of 54.7° (46% of the surface is shadowed by adjacent grooves) results in large geometrical losses and distribution of light over many orders (due to widening of the blaze function with smaller effective groove width). Our calculations indicate that only 28.1% of incident light on the grism should be diffracted into orders and that the rest should be lost in two reflections from silicon surfaces and geometrical

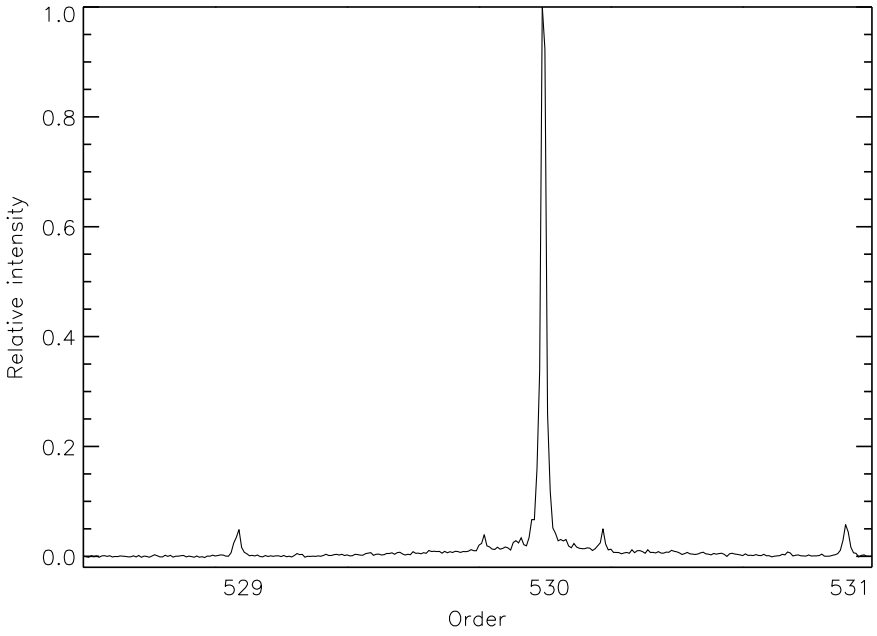


**Figure 3.** Immersion grating spectrum at 1.523 $\mu$m. Scattered light and ghosts are shown in more detail in Figure 6.

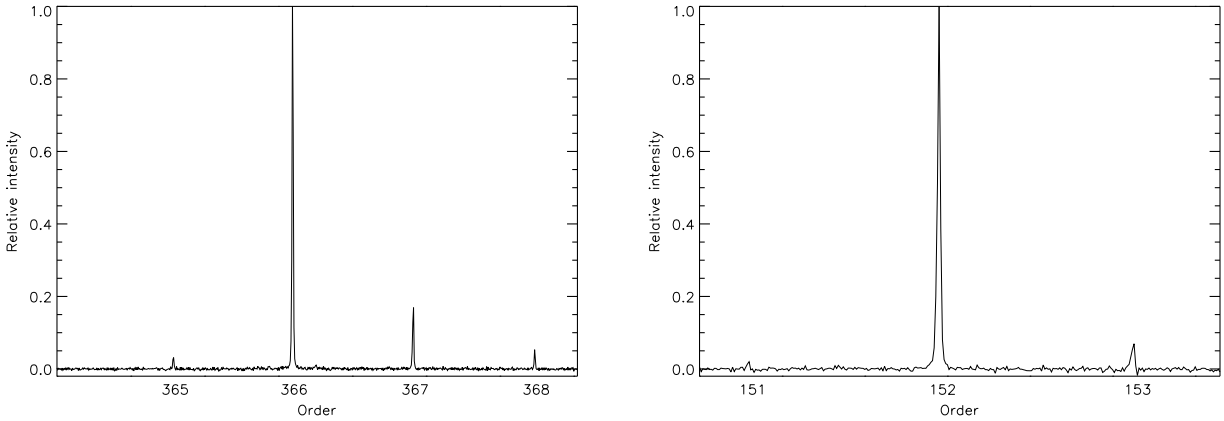


**Figure 4.** Spectrum of the grating used as a front-surface device at 632 nm[1] (left) and 1.523 $\mu$m (right).

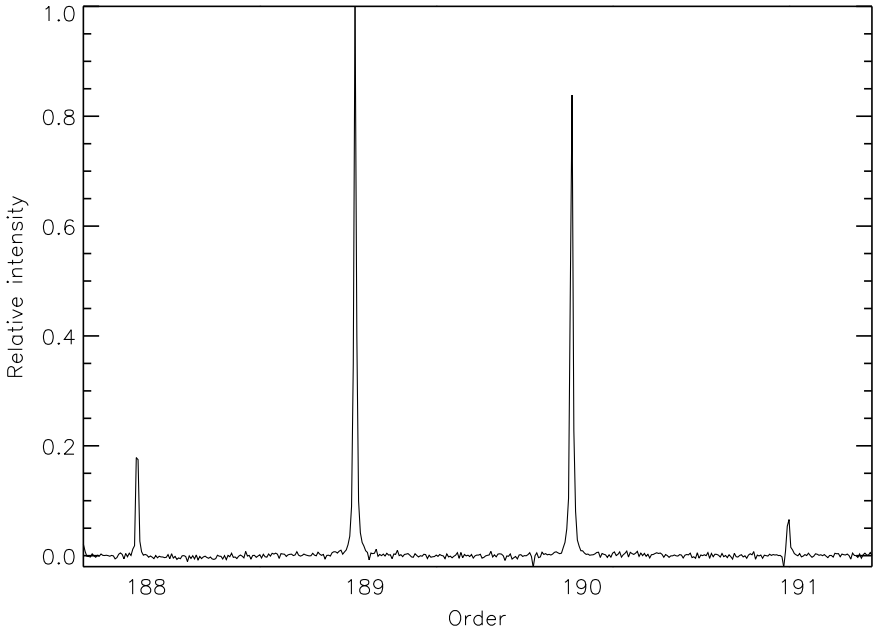


**Figure 5.** Grism spectrum at 1.523 $\mu$m.

shadowing. This shadowing effect becomes much smaller at shallower blaze angles. The relative throughput of our grism is 108% compared to the expected 93.1%. Clearly, the situation where the geometric blockage is very large requires more attention and more careful modeling.

The measured throughput of our grating in immersion was 25.9%±4.7% in three orders (after subtracting out scattered light and ghost contributions). There is no loss in immersion from geometrical blockage. In this mode, the beam undergoes two transmissions and one reflection at uncoated air/silicon interfaces. The maximum achievable throughput is therefore 48.2% relative to the silicon reference mirror. The measured relative throughput in three orders was 53.9%±4.7% in agreement with the predicted 56.8% (again, assuming $\Delta\sigma_{\rm rms}$=37 nm as determined from the front-surface measurements at 632 nm). Another 15.1% is recovered in blazed scattered light and 1.5% in Rowland ghosts (see Figure 6). In immersion, the blaze wavelength is very close to 1.523 $\mu$m and the throughput of our grating on the blaze[5] would be 33%.

The presence of Rowland ghosts (small satellite lines found on each side of the parent spectral line) in the immersion spectrum indicates periodic errors in groove spacing in our case transferred from the photolithography mask. The distance of Rowland ghosts from the parent line is given by[6]

$$\Delta x_{\rm M} = {\rm M}\frac{\lambda}{{\rm P}\,\cos\,\delta}{\rm f} \tag{3}$$

at Littrow incidence where M is the ghost order, P is the period of the spacing error, and f is the focal length of the camera lens. The relative intensity of Rowland ghosts is proportional to the square of the amplitude of the periodic spacing error and for a grating in immersion it is given by[6]

$$\frac{{\rm I}_{\rm ghost}}{{\rm I}_{\rm line}} = \frac{4\,\pi^2\,{\rm n}^2\,{\rm A}^2\,\sin^2\,\delta}{\lambda^2} \tag{4}$$

From the measured distance (22.5 pixels) and intensity (∼2.6%) of Rowland ghosts, we determined the period and amplitude of the spacing error P=780 $\mu$m and A=13.5 nm. The result is very close to the result we got

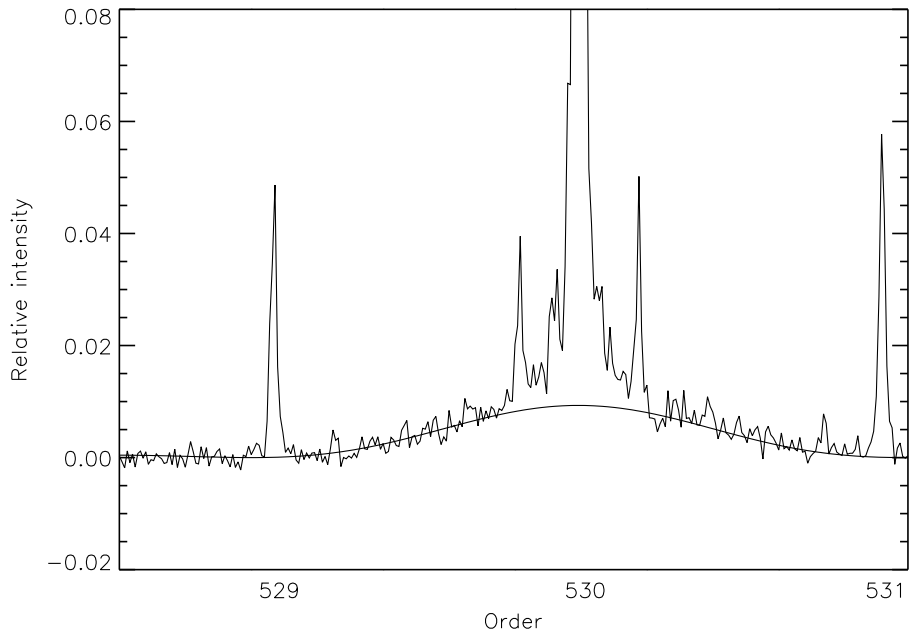


**Figure 6.** Immersion grating spectrum detailing scattered light and ghosts. Rowland ghosts are at a distance of 22.5 pixels from the parent line and their intensity ranges from 2.6% to 8.5% of the parent line. Scattered light has the shape of the blaze and in this case was fitted by the scaled blaze function.

previously,[3] P=726 $\mu$m and A=17.5 nm, using front surface tests ($\lambda$=543 nm) of a grating etched on a silicon wafer. The periodic error causing Rowland ghosts in our spectra is solely the result of using a ruled mask. We have already used new e-beam masks which show no evidence of Rowland ghosts.

Scattered light normally present in a grating spectrum is usually a result of imperfections in groove walls. However, we also find scattered light in the immersion spectrum spread within the envelope defined by the blaze function. Blazed scattered light is most likely due to random errors in groove positions. Presence of both types of scattered light degrade the performance of our grating at 1.523 $\mu$m (which, in immersion, is the equivalent of 437 nm for a front-surface device). One of our primary goals for the immersion gratings project is to produce a device with good performance in the 3–4 $\mu$m band. We therefore modelled the performance of an immersion grating with our current level of groove position error but without the now avoidable repetitive error at 3.5 $\mu$m. Figure 7 shows the result of this calculation. The throughput of this grating on the blaze at 3.5 $\mu$m would be 61% in 227$^{\text{th}}$ order.

## 4. CONCLUSION

We tested a diffraction grating produced by wet etching of a silicon disk and then cut into a prism with the grating covering the hypotenuse side. Leaving the grating uncoated enabled us to test the grating in immersion, reflection and transmission and compare its performance in all three modes. We conclude that the performance of our grating is very close to the performance we expected based on our previous measurements. The errors in groove spacing that degrade the performance of our grating in immersion can be attributed to mask imperfections. We have addressed this problem and are now able to acquire e-beam masks that do not have periodic errors.

## ACKNOWLEDGMENTS

This work was supported by NASA grants NAG5-9230 and NAG5-8858 to the University of Texas at Austin.

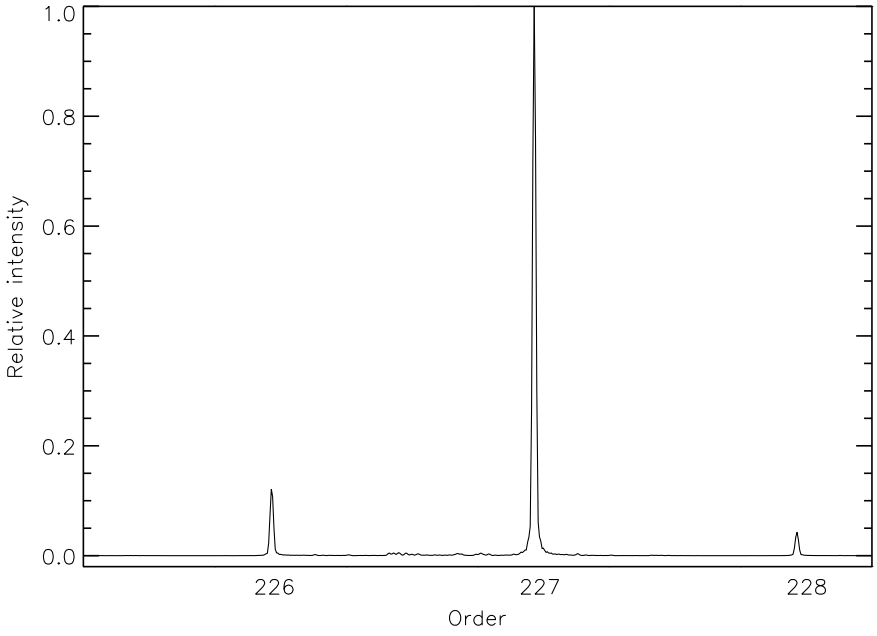


**Figure 7.** Simulated grating spectrum at 3.5 $\mu$m. The intensity of scattered light is significantly diminished and the grating performance is significantly improved.

## REFERENCES

1. O. Ershov, D. Jaffe, J. Marsh, and L. Keller, "Production of high-order micromachined silicon echelles on optically flat substrates," *Proc. SPIE* **4440**, pp. 301–308, 2001.
2. W. Tsang and S. Wang, "Preferentially etched diffraction gratings in silicon," *J. Appl. Phys.* **46**, pp. 2163–2166, 1975.
3. L. Keller, D. Jaffe, O. Ershov, T. Benedict, and U. Graf, "Fabrication and testing of chemically micromachined silicon echelle gratings," *App. Optics* **39**, pp. 1094–1105, 2000.
4. E. O. M. Department, "Germanium and silicon optics," tech. rep., Eagle-Pitcher Technologies, LLC.
5. D. Schroeder and R. Hilliard, "Echelle efficiencies: theory and experiment," *App. Optics* **19**, pp. 2833–2841, 1980.
6. G. Stroke, "Ruling, testing and use of optical gratings for high resolution spectroscopy," in *Progress in Optics, Volume II*, E. Wolf, ed., pp. 3–68, North-Holland Publishing Company - Amsterdam, 1963.